# DETECTION OF HIGH MOMENTUM HADRONS

G. Buschhorn, D. Coyne, J. Cronin, J. Klems,
C. Morehouse, and M. Strovink

## ABSTRACT

An apparatus is described for PEP which will detect, measure, and separate charged hadrons with momenta between 0.75 and 15 GeV/c. We discuss expected rates and consider in detail the various detector elements, including solenoid magnet, track chambers, trigger counters, Cerenkov counters, and time-of-flight system. Backgrounds to the multihadron processes are discussed. A double-arm spectrometer and a toroidal magnet configuration as alternatives to a solenoidal system are briefly considered. A streamer chamber is suggested as a possible alternative for the central detector of the solenoid. Finally, we explore the usefulness of two devices yet to be developed: an efficient relativistic rise detector and a differential Cerenkov counter with large angular acceptance.

## I. INTRODUCTION

We have considered the detection and identification of high momentum hadrons produced in $e^+e^-$ collisions at PEP. The rates expected are very low and a solid angle of $\sim 2\pi$ is required. We describe here a magnetic detector with access in polar angle of 45° to 135° and coverage of 90% in azimuth. Identification of the high energy hadrons ($p > 0.75$ GeV/c, $x > 0.1$ at maximum PEP energy) is done by Cerenkov counters and time-of-flight (TOF). The system will separate charged hadrons into $\pi^{\pm}$, $K^{\pm}$, and $p,\bar{p}$, between 0.75 and 15 GeV/c with the exception of a gap between 3 and 4.6 GeV/c in the separation of K mesons from protons. The proposed system has a diameter of 6.5 m. We have not included muon and electron identification. Inclusion of these features requires an enormous surface area of detector. An additional 2 m in the experimental area should be reserved for installation of such detectors if needed.

Figure 1 shows a schematic view of the detector from one end. The first meter radius is filled with track detectors. Between 1 m and 2 m is the first Cerenkov layer. At 2 m a final track detector is placed. Between 2 m and 3 m the second Cerenkov layer is placed. Finally a layer of trigger scintillation elements is placed at 3.25 m.

Figure 2 shows a schematic view of the detector from the side. For clarity, not all of the Cerenkov detectors are shown.

## II. RATES

While there is an almost complete lack of knowledge of the cross sections and multiplicities for multihadron events at PEP energies, it is helpful to fit various models to the data of SPEAR and to extrapolate them into the new region. This hopefully gives order-of-magnitude results on expected counting rates with subsequent constraints on the proposed detectors.

The extrapolation seems simplest when expressed in terms of the inclusive cross section $d\sigma/dx$ for observation of a single track with $x = E_{hadron}/E_{beam} \geq$ some $x_0$. This absorbs the lack of knowledge of the momentum dependence of the multiplicity behavior (average charged multiplicities vary from 7.5 to 20, depending on model).

Three extrapolations are shown in Fig. 3, where the cross sections have been folded with a projected machine luminosity of $2\times10^{31}$ $cm^{-2}s^{-1}$ to give hourly rates into $4\pi$ steradians. The models used are:

(1) An exponential fit of $s\,d\sigma/dx$ to the curve seemingly approached by SP-2 data as $E_{beam}$ increases.

(2) A power-law fit of $E/p^2\,d\sigma/dp$ to the high x data, assuming the invariance under s of such data on this and the $s\,d\sigma/dx$ plots implies a $1/p^4$ or $1/x^3$ dependence [ due to Auerbach].

(3) An exponential fit of $1/E_{beam}p\,d\sigma/dp$ vs p following the thermodynamic model of Engels et al. in which the momentum dependence is absolute.

All these models are constrained to the kinematic limit that $x \leq 1$. The first two show a $1/s$ dependence that cancels the assumed s dependence of the luminosity, while the third does not. The first two give good and equivalent fits to SPEAR data, the third gives a rather poor fit. We note that a

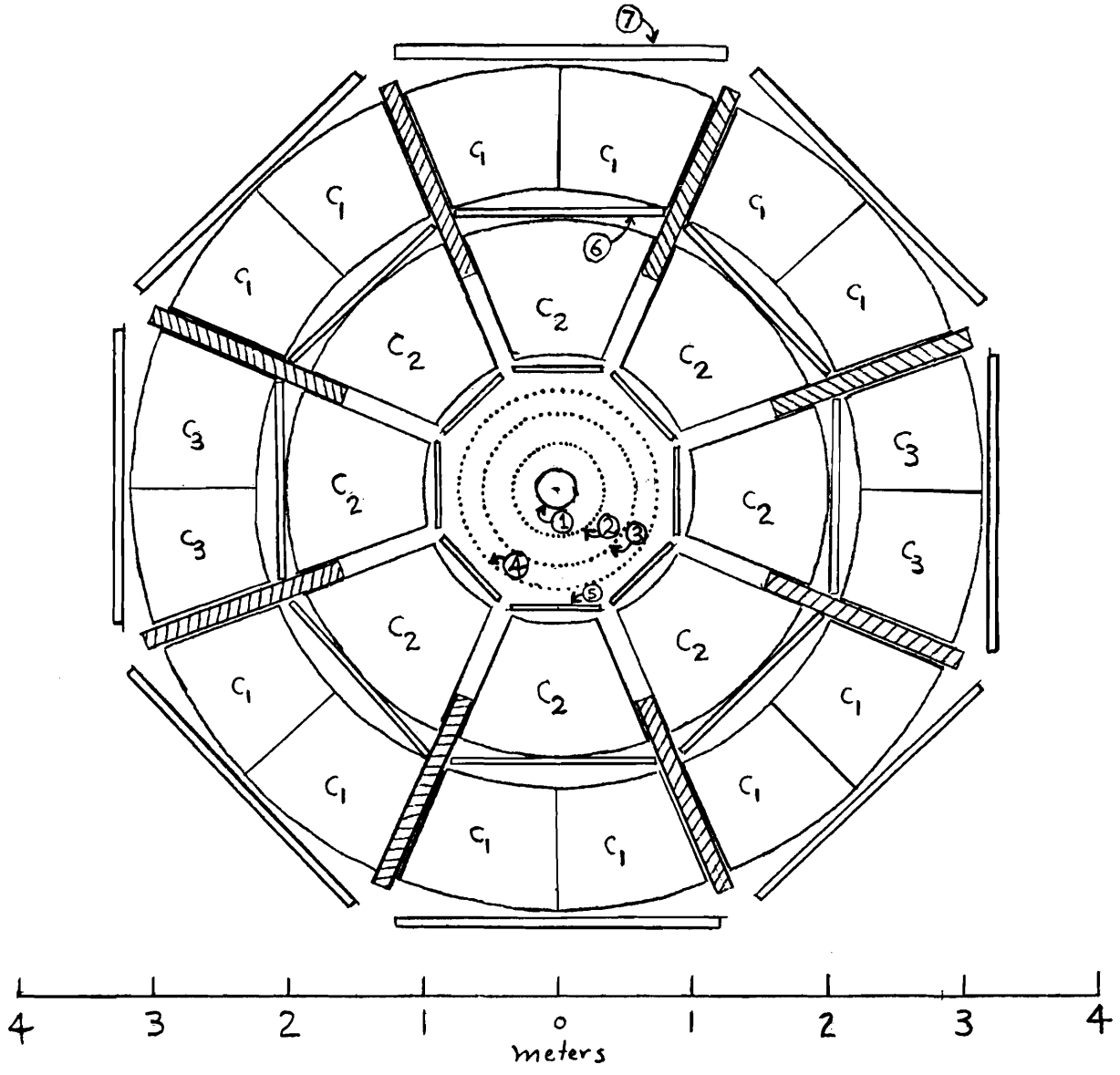


Track Chambers and Scintillators

| | |
|---|---|
| ① | High Pressure MWPC |
| ②③④ | Spark Chamber |
| ⑤ | Drift Chamber ($\varphi$) |
| | Coarse MWPC ($\theta$) |
| ⑥ | Drift Chamber |
| ⑦ | Trigger Scintillator |

Cerenkov Counters

| | |
|---|---|
| $C_1$ | 1 atm $CO_2$ |
| $C_2$ | 1 atm pentane |
| $C_3$ | 6 atm propane |

Fig. 1. High-momentum hadron detector (end view).

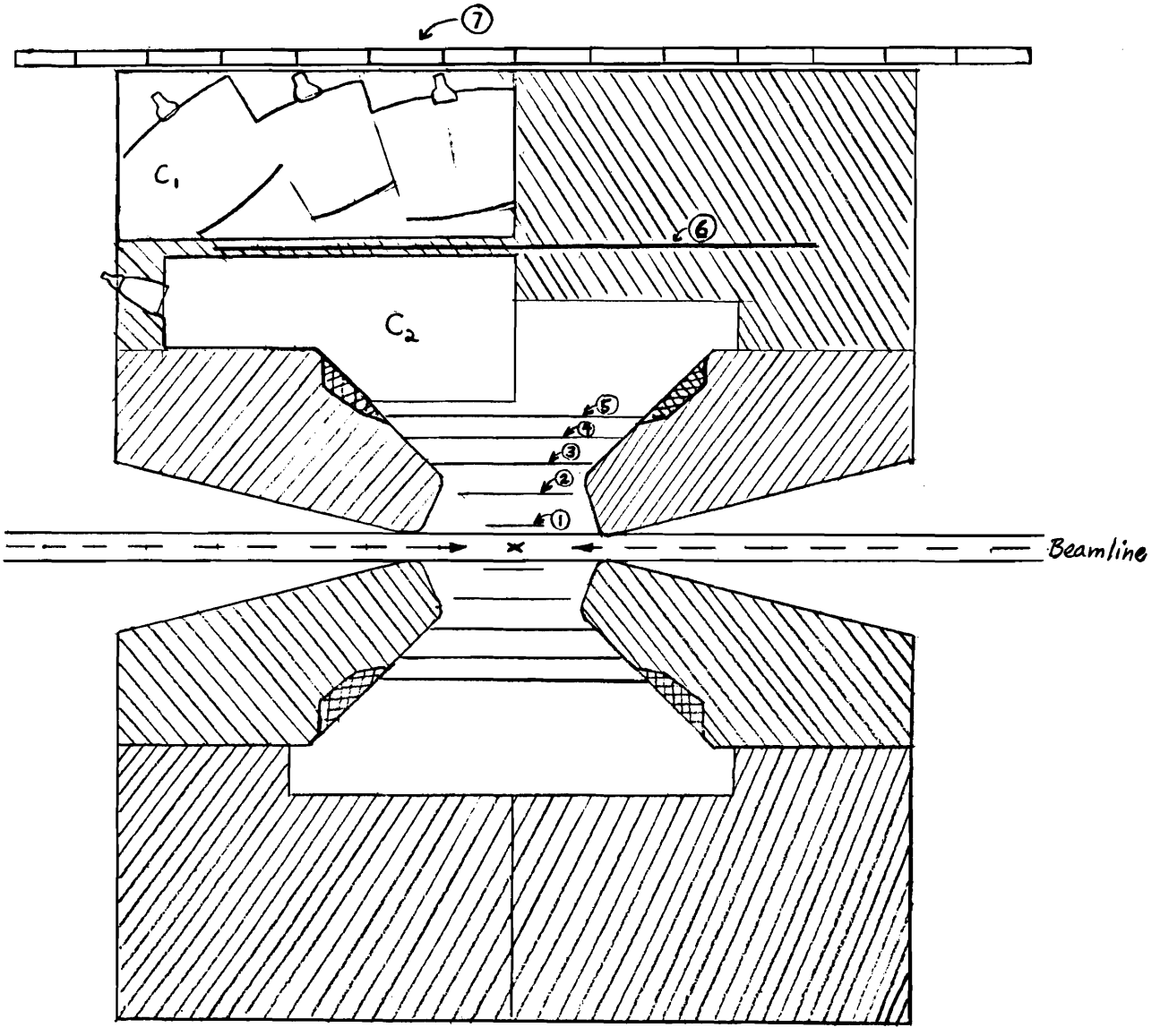


Fig. 2. High-momentum hadron detector (side view).

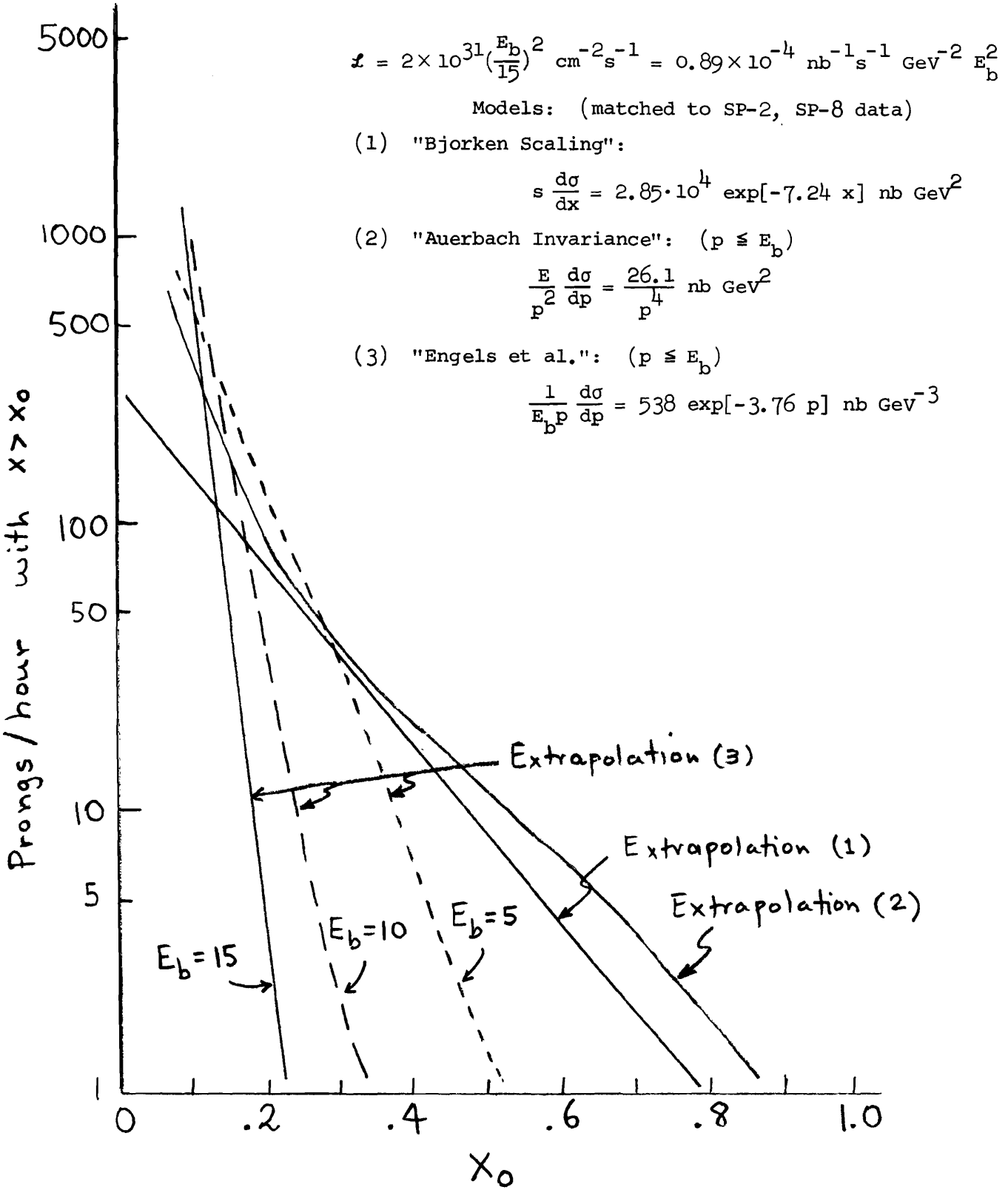


Fig. 3. Rate extrapolations for PEP energies. $E_b$ is single-beam energy; E is particle energy. Models (1) and (2) are independent of $E_b$, whereas (3) is not.

fourth extrapolation, Richter's combination exponent and power law fit to $s\,d\sigma/dx$, is equivalent within about 10% to model (1) above.

Typical "optimistic" (excluding further marked increase of R) estimates for a 1000 hour run at the "standard" $0.25\times10^{32}$ $cm^{-2}sec^{-1}$ luminosity are then

$$\int \mathcal{L}dt = 0.9\times10^{38}cm^{-2} \begin{cases} x > 0.1 & 2\times10^{5} \text{ tracks} & 2\times10^{4} \text{ events} \\ x > 0.5 & 1\times10^{4} & 5\times10^{3} \\ x > 0.9 & 6\times10^{2} & 6\times10^{2} \end{cases}$$

The last column is a crude estimate of the number of actual unique events. All of this is for a 100% efficient $4\pi$ detector.

Conclusions: Extrapolations do not give an order-of-magnitude confidence unless the more extreme models are discarded a priori. Even with the optimistic estimates a large-x detector should include an appreciable fraction of $4\pi$ steradians. The added uncertainty of the product (physics × machine performance) implies that a good deal of effort to optimize this detector is justified.

## III. DETECTOR

### A. Magnet

Momentum-analysis of the charged secondaries is of special importance in this spectrometer because of the emphasis on high hadron momentum and because of the necessity to measure both momentum and velocity in order to identify the particle type. A spectrometer magnet was designed with the help of Dr. Klaus Halbach of LBL for this purpose, with the constraints: (1) no components of the magnet lie at any radius within $\theta < 15°$, $45° < \theta < 135°$, $\theta > 165°$, and within 90% of the azimuth—i.e., an "open" configuration; (2) beyond 2 m of the beam axis, low fringe fields permit easy magnetic shielding of Cerenkov phototubes; (3) within $45° < \theta < 135°$ and within 0.5 m of the beam axis, the magnetic field is solenoidal and uniform to about 10%; (4) field strength and extent permit adequately precise momentum measurement (elucidated below). In addition, large size and cost were to be

avoided to the extent possible.

A representative but not optimized conceptual design for this magnet is shown in Fig. 4. The figure depicts one quadrant of a section of the cylindrically symmetric magnet in a plane containing the beam axes. Moderate field levels permit extensive use of iron to shape and return the flux. This iron takes the form of pole pieces with boundaries lying on conical surfaces, and of 8 flux-return "vanes," one per octant, occluding 10% of the azimuth. These vanes are the distinctive feature of the magnet. In addition to returning the flux, they short out the fringe field, which damps at distance L within the vanes as $e^{-\pi L/D}$, with D the vane separation. The vanes also serve as very rigid support structures for high-precision track-measuring planes, and as heavy walls for pressurized Cerenkov counters. Since the vanes subtend only 10% of the azimuth, they are easily saturated unless protected from stray flux by properly shaped pole faces, as shown.

The magnet leaves open a solid angle of approximately 65% of $4\pi$ steradians. The indicated flux map was generated by a relaxation calculation assuming infinite permeability in the iron, where fields generally do not exceed 18 kG. The calculation predicts a central field of 8.1 kG at excitation of $3.6\times10^{5}$ A-turns/coil, corresponding to 0.5 MW of power consumed by coils of total weight 5 tons. The yoke weight is 230 tons. Without a detailed engineering estimate it is hoped that the magnet cost lies in the neighborhood of $250K.

The momentum resolution achievable with a field configuration of this type is worst within the range $45° < \theta < 135°$ at the midplane $\theta = 90°$. The magnetic field shape at the midplane is also shown in Fig. 4. With measuring planes having $r\sigma_\phi = 0.2$ mm located at r = 0.15 m, 0.9 m, and 2.1 m (see below), the midplane momentum resolution is given approximately by

$$\frac{\sigma_p}{p} \approx 6\times10^{-3}\ p\ (\text{GeV}),$$

and is roughly inversely proportional to the midplane integral

$$\int_{0.15\text{m}}^{1\text{m}} (r - 0.15\,\text{m})B(r)dr,$$

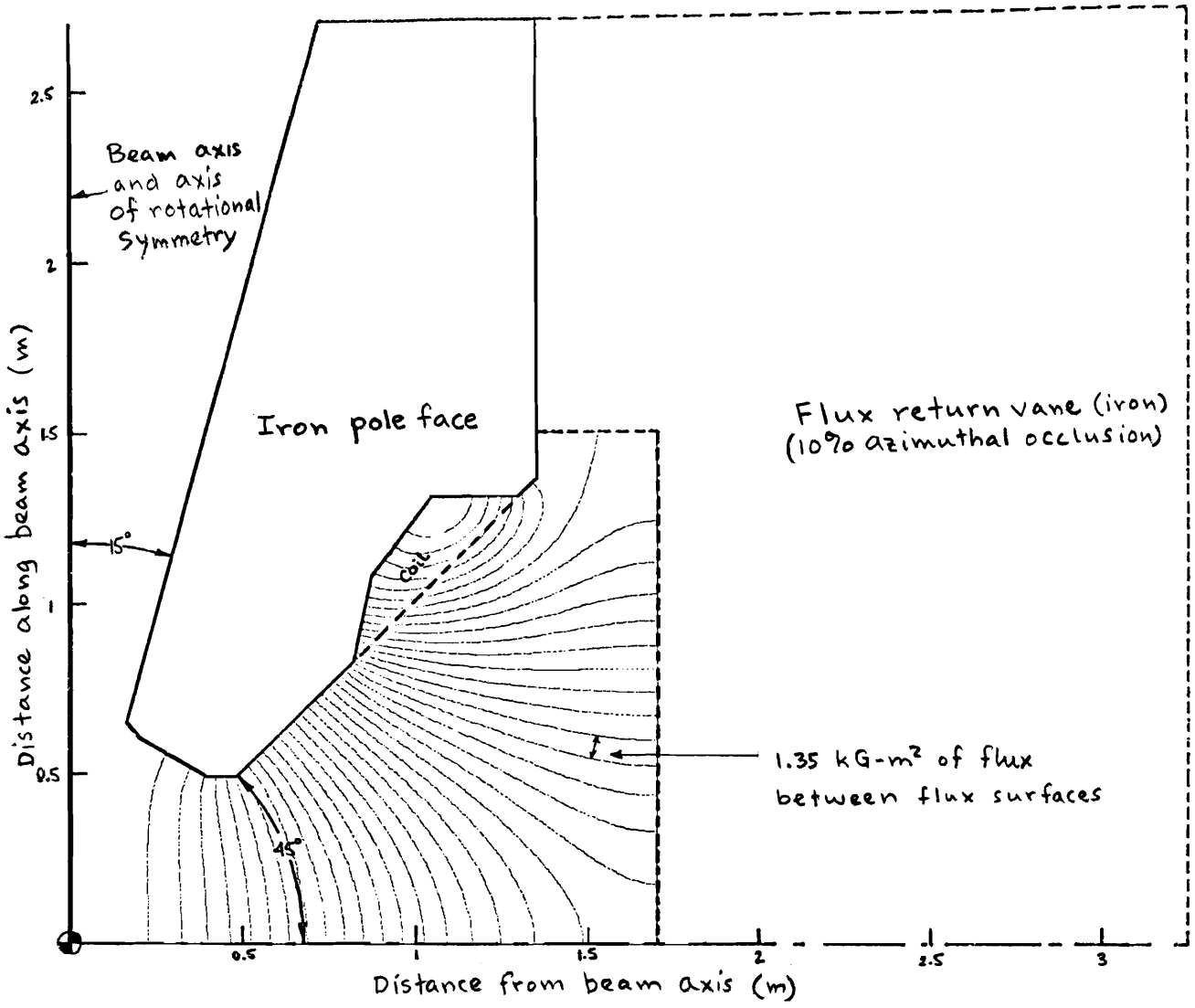


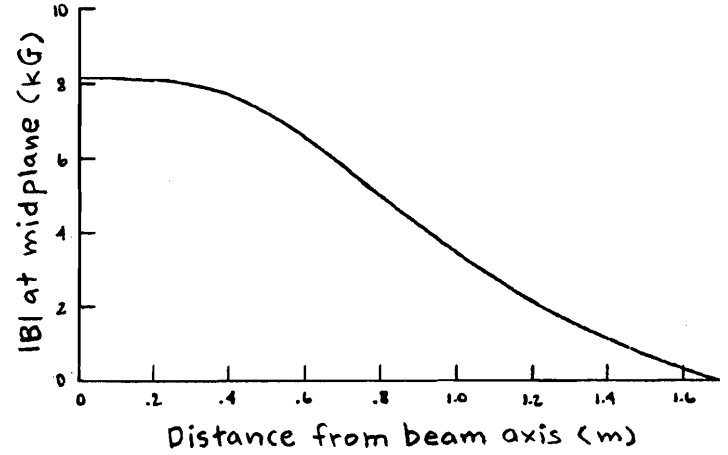


MAGNET PARAMETERS (approximate)

| | |
|---|---|
| Excitation | $3.6 \times 10^5$ A-T (each coil) |
| Coil | 1 kA/cm$^3$ of Cu |
| | packing fraction 0.5 |
| | weight 2.5 T (each) |
| | power 0.25 MW (each) |
| | 0.5 MW (total) |
| Yoke | length 5.4 m |
| | diam. 6.5 m |
| | weight 230 T |
| Rough Costs | coil $100 K; yoke $150 K |

Fig. 4. High-momentum hadron detector: solenoid magnet and field configuration.

which is 2.3 kG-$m^2$ in this design. This momentum resolution corresponds to $\Delta p/p = 6\%$ at $p = 10$ GeV/c. As an example of its effect on the observed spectrum in $x = 2p/\sqrt{s}$, we suppose that $d\sigma/dx \propto e^{-7.24x}$ at $x = 2/3$ (see below), and approximate $\sigma_x = 0.04$ in that region. In this case the observed rate at $x = 2/3$ will be $e^{(7.24(.04))^2/2} = 1.043$ times the true rate due to smearing. This smearing factor becomes $\approx 1.2$ if the resolution should worsen by a contingency factor of 2.

## B. Track Chambers

The table inset on Fig. 1 lists the track detectors envisioned. We describe them briefly, referring to the numbers indicated in Figs. 1 and 2.

Detector (1) is a high pressure multiwire proportional chamber (MWPC) with 0.5-mm wire spacing in the azimuth. In addition the cathodes are used by induced signal to measure the z coordinate separated into four quadrants. The resolution in z (standard deviation) is ~ 0.2 mm.

Detectors (2), (3), and (4) are spark chambers with individual wire readout (capacitive storage with shift register read out, for example). Each module consists of two gaps of wires with small-angle stereo in the style of the SPEAR magnetic detector. (The total number of wires is ~ 42 K.) These detectors do the hard work of tracking and disentangling the expected high-multiplicity events in the central region. The mechanical design and extraction of information from these chambers in the tight space will be difficult and some otherwise useful solid angle may be consumed in the process. It was felt important for symmetry tests that the magnet be readily reversible, a process difficult with magnetostrictive readout.

Detector (5) is a drift chamber in the azimuthal coordinate with 1-cm wire spacing. Its resolution is estimated to be 0.2 mm. In the z coordinate the detector is a MWPC with 3-mm wire spacing. These wires are ganged by 4 to give 1.2-cm elements. These elements, coupled with scintillators at the outer radius, provide the trigger. There are eight such detectors.

Detector (6) is a drift chamber with 2-cm wire spacing in azimuth and 4 cm in z. Its azimuthal resolution is estimated to be 0.2 mm. There are eight such detectors.

The momentum determination is made by detectors (1), (5), and (6), and should be adequate to determine the momentum of a 10-GeV/c track with a standard deviation less than 10%.

Detector (7) is a bank of trigger scintillators. In each octant one has 14 $0.1 \times 0.5 \times 2.5$ m liquid scintillators. A photomultiplier on each end provides a position-independent time measurement for a detected particle.

Table I summarizes the properties of the track detectors.

## C. Triggering

We plan to use a single particle trigger. The idea is to use the fact that in a $\theta$ projection the track appears straight. The principal trigger elements are the scintillators (7) (gated by a beam crossing) and the MWPC (5). For both (5) and (7) the eight octants of fixed $\theta$ are placed in OR. The two signal sets feed into a matrix coincidence. Elements of the matrix corresponding to tracks extrapolating to the interaction region are chosen to trigger the spark chambers and latch all information.

## D. Cerenkov Counters

We assume that Cerenkov techniques are to be used to identify high momentum charged hadrons. We can try to specify the "ideal" system of Cerenkov counters to tag uniquely pions, kaons and protons in the PEP energy range. Such a system could consist of three threshold Cerenkov counters used in tandem. (Differential Cerenkov counters are not considered because large solid angle complicates the optics of such counters.) The following chart indicates how the three counters are used in identification.

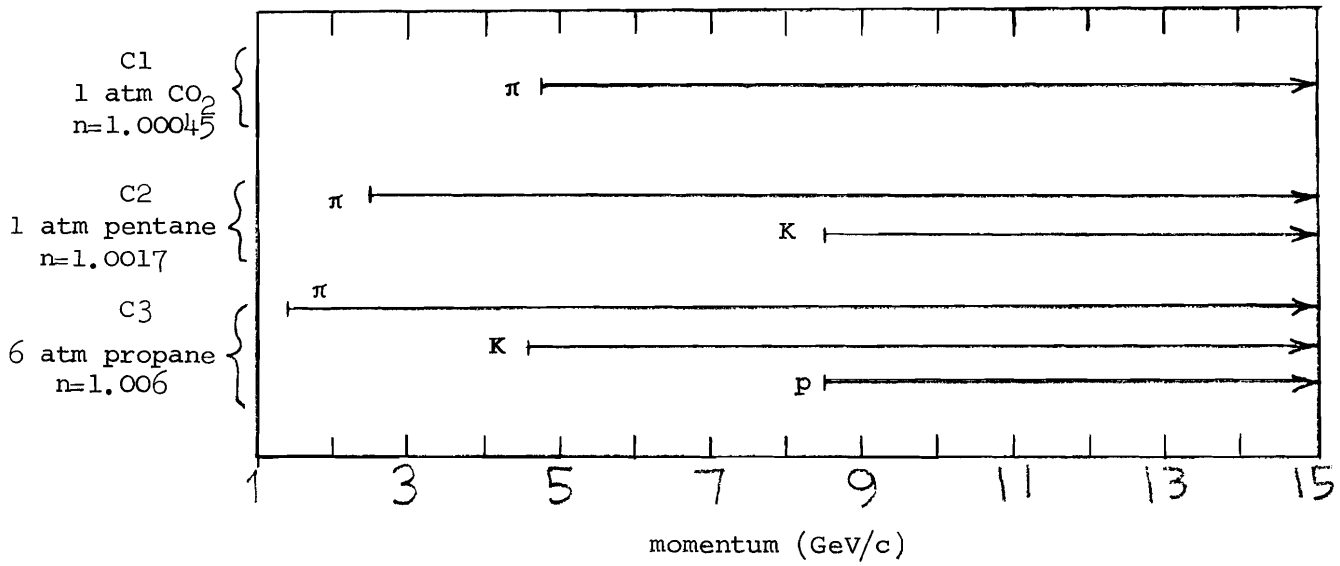

Table I. Track chambers for PEP high momentum hadron detector.

| Device | | Mean radius (cm) | Length (cm) | Azimuth ($\phi$) | | z Coordinate | | Number of channels | |
|---|---|---|---|---|---|---|---|---|---|
| | | | | Wire spacing | Resolution | Wire spacing | Resolution | $\phi$ | z |
| High pres. MWPC | (1) | 15 | 40 | 0.5 mm | 0.2 mm | ~4 mm | ~2 mm | 1 884 | 400 |
| Spark chamber | (2) | 36 | 80 | 1 mm | 0.5 mm | Small-angle stereo | ~1 cm | 9 040 | --- |
| Spark chamber | (3) | 56 | 112 | 1 mm | 0.5 mm | Small-angle stereo | ~1 cm | 14 064 | --- |
| Spark chamber | (4) | 76 | 152 | 1 mm | 0.5 mm | Small-angle stereo | ~1 cm | 19 088 | --- |
| Drift chamber | (5) | 90 | 180 | 1 cm | 0.2 mm | --- | --- | 560 | --- |
| MWPC | (5) | 90 | 180 | --- | --- | 3 mm ganged by 4 | 1.2 cm | --- | 1 200 |
| Drift chamber | (6) | 205 | 420 | 2 cm | 0.2 mm | 4 cm | 0.4 mm | 560 | 840 |

From the chart, one can see that, given any momentum above 4.6 GeV/c, there is a unique tag for pions, kaons, and protons.

Whereas the triple-tandem counter system is in principle the tagging system we want, practical considerations force us to use only two counters simultaneously. The combinations we propose are the C1-C2 combination in six octants and the C2-C3 combination in two octants. From the chart it is seen that the C1-C2 combination separates pions from K's and protons above 2.5 GeV/c and gives $\pi$-K-p tagging above 8.5 GeV/c. The C2-C3 combination separates pions from K's and protons between 1.4 GeV/c and 8.5 GeV/c, gives $\pi$-K-p tagging from 4.6 GeV/c to 8.5 GeV/c, and separates protons from pions and kaons above 8.5 GeV/c.

The physical characteristics of the three counters are determined largely by the Cerenkov angle in the counter. Assuming first that the number of photoelectrons is given by

$$N_e = 50\ L\theta^2\ , \qquad \text{where } L \text{ is in cm,}$$

we calculate $N_e \approx 4$ per meter in the $CO_2$ counter. We thus fix the depth of the $CO_2$ counter (C1) at 1 m. This counter is shown in Fig. 5. We propose to mount this counter on the outside of the quadrants in which it is mounted (six quadrants). This counter has 12 5-in. PM tubes per octant.

Structurally the most difficult counter is C3 ( 6 atm propane), which is shown in Fig. 6. We propose to use the iron flux return vanes as structural members and enclose mirror boxes in one large pressure vessel. The light production is no problem, $N_e \approx 40$ for 50 cm counter. The optical problem here is to reduce the large effective source size to phototube size. A total of 12 5-in. PM tubes per octant will collect the light.

The inner counter in each octant (C2, shown in Fig. 7), is designed to be filled either with $CO_2$ or pentane. The major difficulty is efficient collection and transmission of light around the pole piece of the magnet. For this counter 4 5-in. PM tubes per octant are used to collect the light. Part of the light in C2 suffers four reflections and some high quality mirrors ($M_1$ and $M_4$ in the sketch) will be required.

In total, 16 5-in. PM tubes are required per octant (irrespective of the counter combination), leading to 128 5-in. PM tubes total (for example, 4522). Table II shows the photomultipliers required for the Cerenkov counters, the trigger counters, and the TOF counters described in the next section.

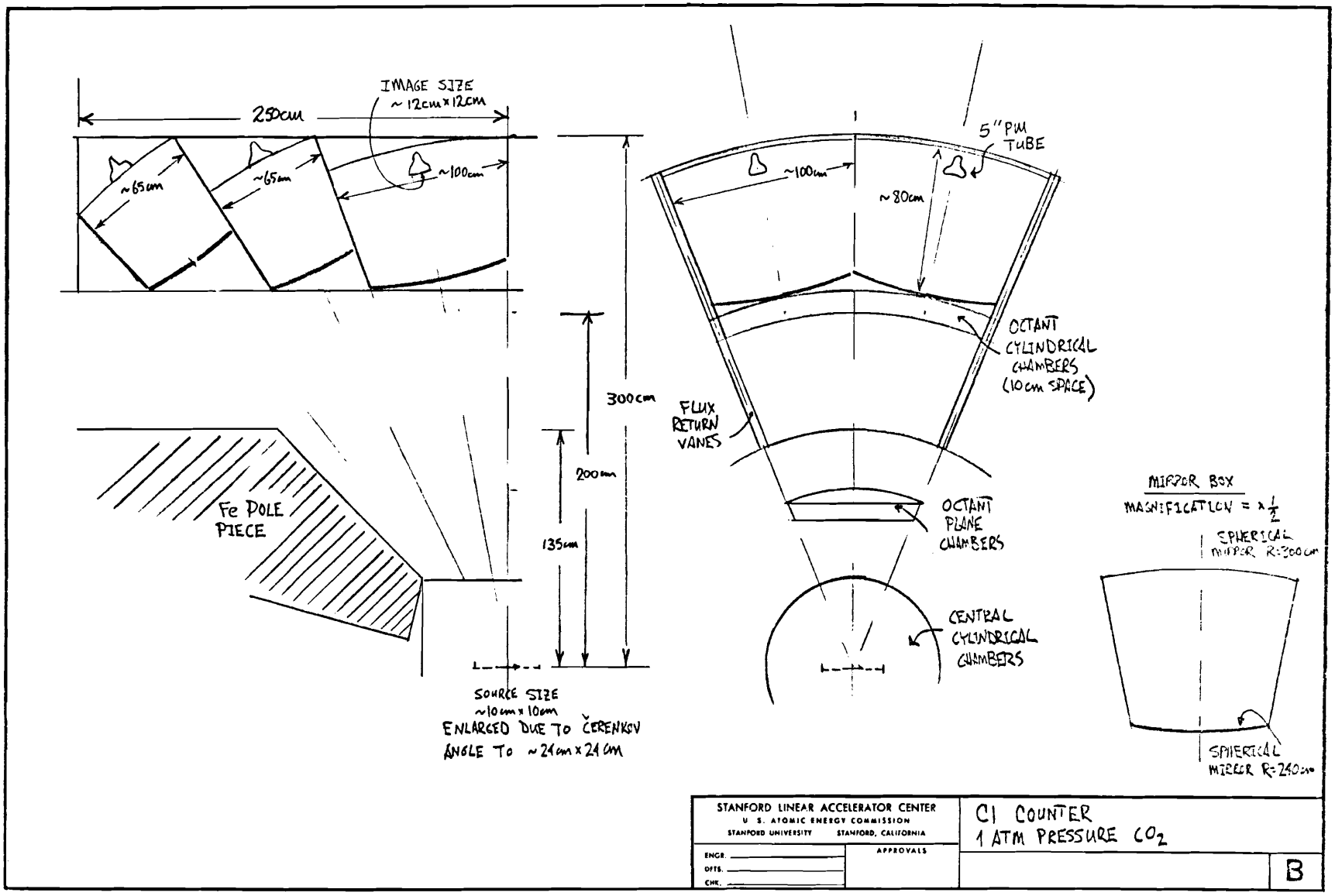


Fig. 5. High-momentum hadron detector: details of C1 Cerenkov counter.

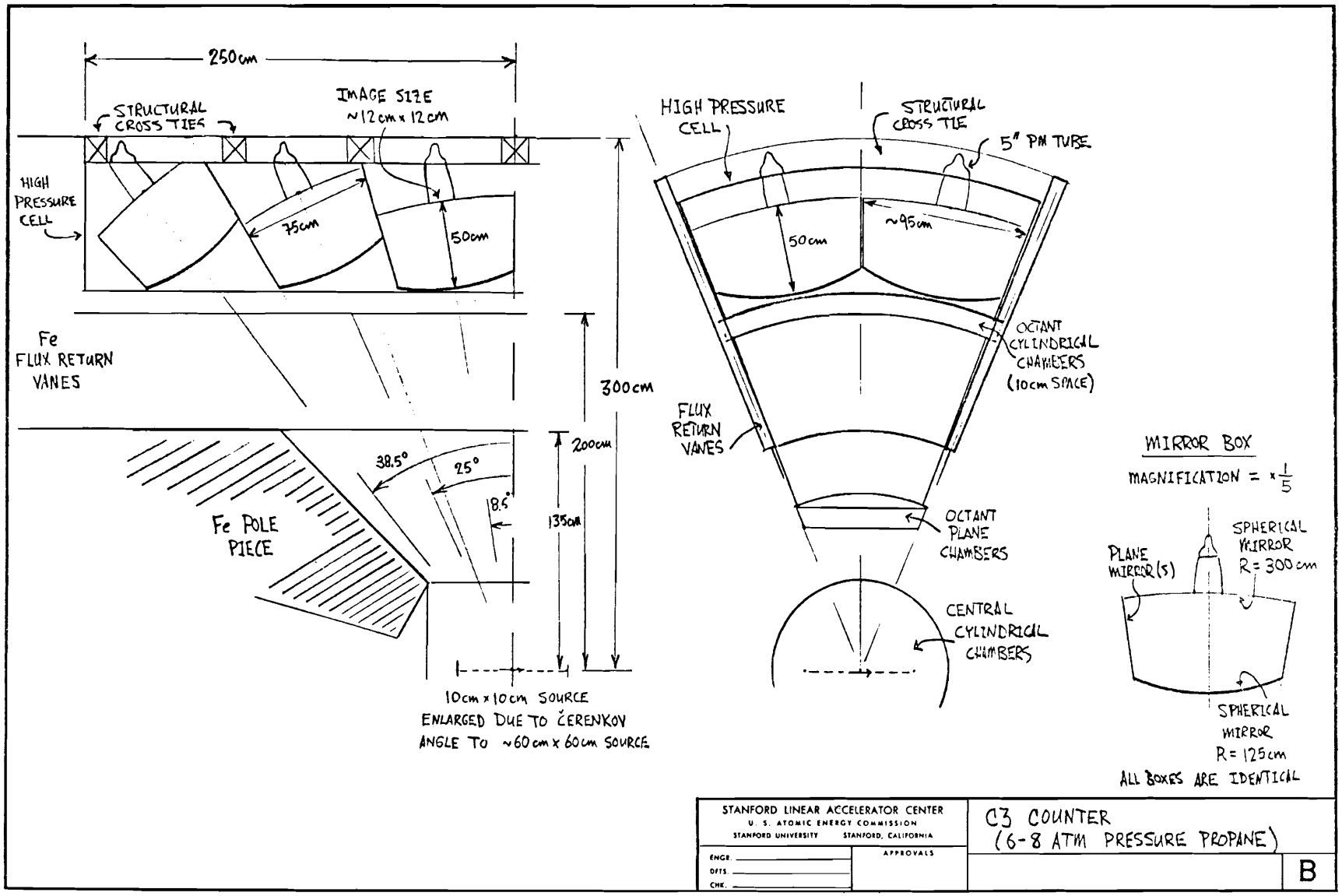


Fig. 6. High-momentum hadron detector: details of C3 Cerenkov counter.

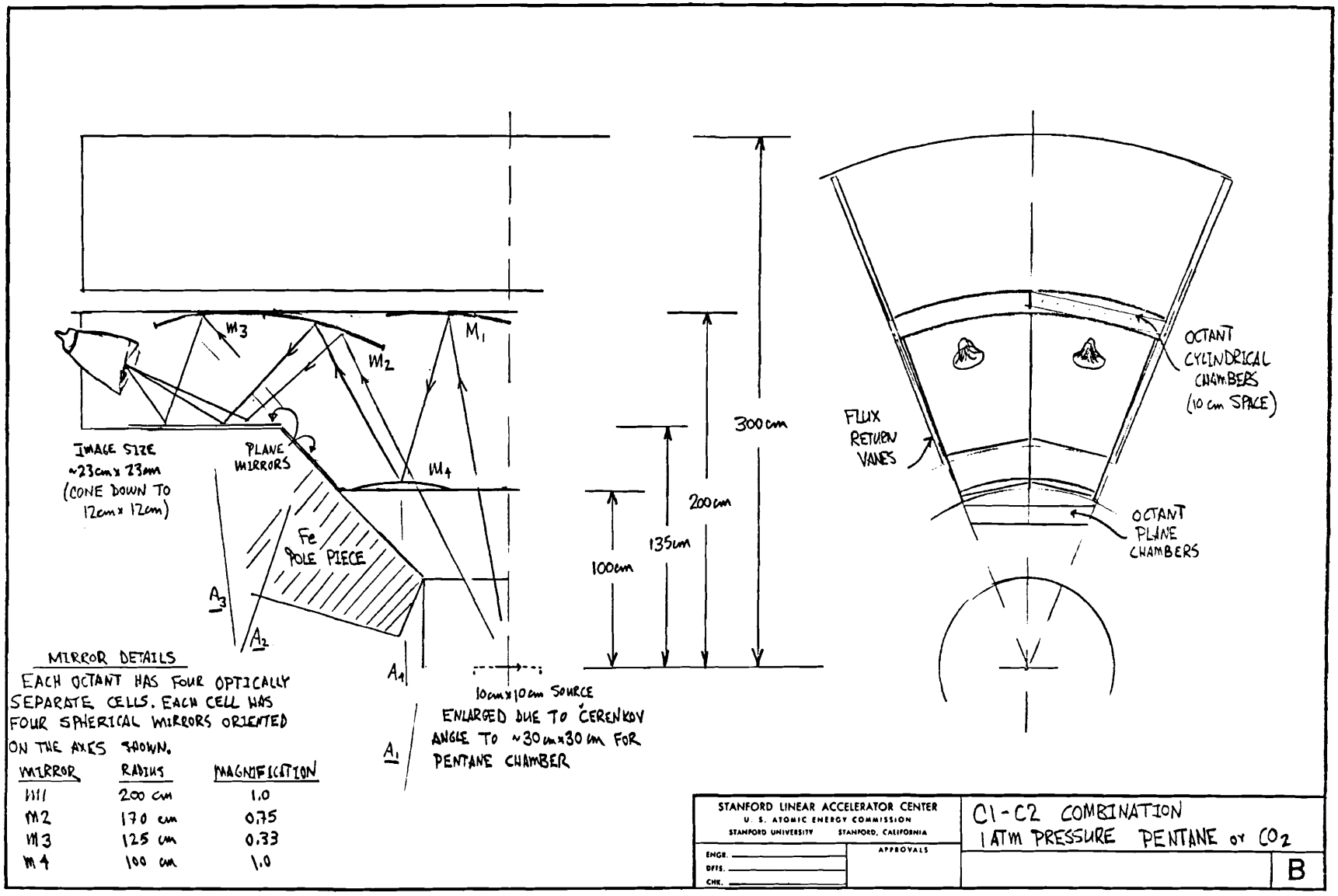


Fig. 7. High-momentum hadron detector: details of C1-C2 Cerenkov counter combination.

Table II. Photomultiplier summary.

| Detector | Number | PM/D | Total PM |
|---|---|---|---|
| C1 | 12 | 6 | 72 |
| C2 | 16 | 2 | 32 |
| C3 | 4 | 6 | 24 |
| | | Total 5-in. high-quality tubes | 128 |
| Trigger | 112 ($140\ m^2$) | 2 | 224 |
| 6 meter TOF (1 octant) | 56 ($70\ m^2$) | 2 | 112 |
| | | Total 2-in. tubes | 336 |

## E. Time-of-Flight Measurement

In the momentum range $p < 1\text{-}2$ GeV/c, where most of the hadrons are expected, they can be identified rather well by TOF measurement. Clearly it would be advantageous to have a TOF system that covers completely the momentum range below the onset of Cerenkov separation. However, since K-p separation by C3 starts only at $p \approx 4.6$ GeV/c, even for a time resolution $\Delta\tau \approx 0.5$ nsec, a prohibitively large TOF path of ~10 m would be necessary. A more realistic approach is to use, for 6 of 8 octants, the trigger counters (at a radial distance of 3.25 m) for TOF separation and for 2 octants to move the TOF counters further out in order to minimize the gap in which hadrons cannot be identified. For $\Delta\tau \approx 0.5$ nsec FWHM and 2.4 $\sigma$ separation, one obtains, for example, at:

r = 3.25 m (trigger counters)
$\pi$ - K separation for $p < 1.5$ GeV/c
K - p separation for $p < 2.6$ GeV/c

r = 6 m (outer TOF counters, $2 \times \frac{\Delta\Omega}{4\pi} \approx 0.14$)
$\pi$ - K separation for $p < 2.1$ GeV/c,
K - p separation for $p < 3.6$ GeV/c
(total area $\approx 70$ m$^2$, total number of photomultipliers $\approx 112$).

## F. Background

For the solenoidal detector presented here, with the trigger as previously described, we expect the following backgrounds to the true $e^+e^- \rightarrow$ multihadron process.

1. Alternative processes.

1) QED. The expected number of $e^+e^- \to e^+e^-$ and $e^+e^- \to \mu^+\mu^-$ is ~ 80/h and 8/h, respectively, for an effective luminosity of $2.5 \times 10^{31}$ $cm^{-2}$ $sec^{-1}$. With the smearing of the measured x (normally 1.0) of about 20% due to radiative corrections and momentum resolution, it is clear that this rate will swamp the real multihadrons expected above $x \approx 0.9$. Separation then depends on recognition of the hadronic event by its multiplicity and coplanarity characteristics. Shower counters or hadron filters might be necessary to separate multiplicity-2 events above $x = 0.9$.

2) 2γ process. The $(\ln E_b/m_e)^2$ term in the 2γ cross section ($e^+e^- \to e^+e^-$ + hadrons) increases by only a factor of +2 from SPEAR to PEP energies. The rates for $e^+e^- \to e^+e^-\pi^+\pi^-$ (for a pion form-factor = 1) have been calculated and show that this rate is $10^{-2}$ of the projected multihadron rate. The inclusive rate ($e^+e^- \to e^+e^-$ hX) is potentially larger than the projected $e^+e^- \to$ hX rate, but is damped by a $1/s_h^2$ factor ($s_h$ = [hadronic energy]$^2$). The combination of polar angles > 45° and an $s_h$ of the order of 50 $GeV^2$ should give 2γ rates no worse than the ≈10% seen at SPEAR. Only if there were a class of very low x (≈ 0.1) events with low charged multiplicity (i.e., mostly neutrals) should serious competition occur, since the $s_h$ cut could not be applied.

3) Exotic process. The production of any intermediate state leading to leptons in a final multihadron state is undetectable since this detector has no e or μ separation.

2. Environmental processes.

1) Cosmic rays. With a trigger requiring a single track originating from the central chambers, timed with the rf within a 30-ns window, and projecting linearly (in θ) to an external chamber, we expect a cosmic accidental rate of about 300/h.

2) Machine associated spray. While really unknown for PEP, extrapolations based on currents and lifetimes indicate that PEP should be no worse than about 5× SPEAR in its close-to-beamline background rates into 4π steradians. PWC's touching the 6-in. diameter beam pipe at SPEAR I ran at 10-50 kHz into ~ 4π steradians under normal conditions. This background diminished rapidly with increasing radius but was not reduced

by placing an Al shield around the beam pipe. There is some indication from this and from SP-2's end cap chambers that this background is in part a sheath around the pipe of small angular divergence. Its energy spectrum is unknown. While the overall rates in the inner detector of the proposed detector for PEP do not look serious, the effect on these chambers of the orbital motion of the background in the ~ 8-kG field near the pipe is unknown.

3. Conclusions

While the general functioning of the detector for $0.1 \lesssim x \lesssim 0.9$ would not seem degraded by these background rates, there are particular functions which can be carried out only if additional equipment modules are added (perhaps at a later time). In particular, below $x = 0.1$ a monitor on the $2\gamma$ rate would be advisable. An aperture in the magnet pole has been left for such tagging. Small shower-chamber modules placed at ± 5 m from the interaction point, adjacent to the beam pipe, should sample this rate at $e^{\pm}$ angles > 30 mr, where a small but detectable portion still exists ($\approx 25\%$). Limited shower counter modules and/or hadron filters are required for some topologies with $x > 0.9$ and for "exotic" physics. With fields close to the beam-pipe one should at least be prepared for the innermost track chamber operating in a noisy environment.

## IV. ALTERNATIVE TECHNIQUES

The axial field detector described above might be compared with other choices for the magnet configuration or the detection method.

### A. Double Arm Spectrometer

A very simple detector could employ a single dipole magnet (as in the Maryland-Princeton-Pavia experiment at SPEAR) or two dipoles on opposite sides of the beam (for example, the DASP system at DORIS). Two dipoles of opposite polarity offer the advantage that the beam region to first order remains field free and the distance of the magnets from the beams can be made small in order to achieve a large solid angle. Similar to the DORIS-double-arm spectrometer, the inner field-free region of the double magnet system can be filled with charged/neutral detectors covering a large fraction

of $4\pi$, while good momentum resolution and particle identification is achieved only for the much smaller part of the solid angle covered by the magnet aperture. Pushing a double-arm spectrometer to its limits, it appears to be possible to achieve an acceptance of $\Delta\theta \approx \pm 50°$ and $\Delta\phi \approx \pm 16°$, corresponding to a total solid angle of $\Delta\Omega \simeq 2$ sr. An integral field of 7.5 kG-m would allow then for a momentum resolution $\Delta p/p \approx 10\%$/at 10 GeV/c. The required magnet power would amount to 0.6 MW.

While a double-arm spectrometer offers the advantage of simple geometry and large flexibility, its main disadvantage in comparison to an axial or solenoidal field detector is that it provides momentum analysis of charged particles over a substantially smaller part of the solid angle only. Under the assumption that only about 50% of the useful solid angle of a solenoidal detector can be covered with particle-identifying counters, the effective solid angle of a double-arm spectrometer would be smaller by a factor of about 3.

## B. Toroidal Magnet

As with any such instrument, the solenoidal detector, which is the main design thrust of this report, contains certain compromises. The question arises as to whether alternative magnetic geometries relax these constraints, and what new compromises such geometries involve.

The major constraints of the solenoidal design are:

1) Lack of field-free region around beam pipe (this might be still possible in a scaled-up solenoid).
2) Cutoff in polar angle at 45°.
3) Complexity of Cerenkov optics and loss of differential information.
4) Lack of easy access to "impacted" central chambers.
5) Absence of shower counters and hardon filters due to radial scale of detector.

Comparison of this design with a toroidal field has been done, but in much less detail than the main design itself. The configuration is an eight-pole magnet with long iron segments allowing a minimum polar angle of 30°. The field has a $1/r$ dependence with a mean of 2 kG. (See Fig. 8.) The inner 1 m of detector is essentially field free. Azimuthal transparency is ~2/3. The magnet runs at ~2 MW with Cu coils of 100 $cm^2$ cross section. Cerenkov counters and shower counters and/or hadron filters are placed beyond this magnet in radius, but no specific design studies have been done.

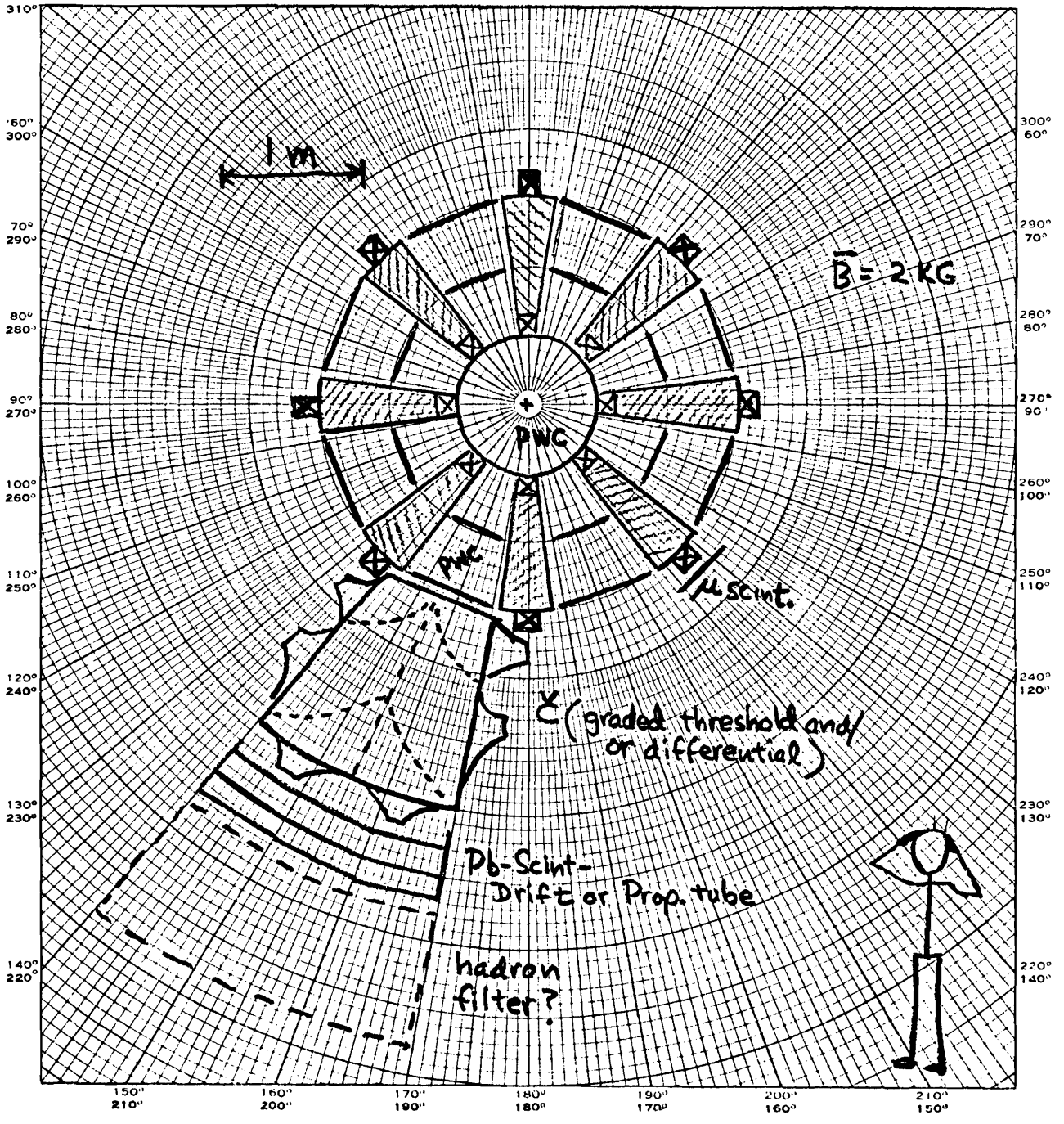


Fig. 8. Toroidal magnet configuration (end view).

A system such as this helps a great deal in removing constraints 1), 2), and 4) above. It may well help problem 3) since a good deal of open space is adjacent to each Cerenkov. The differential information is retained in that the "natural" line source of particles is maintained under curvature of particles in the field. Problem 5) becomes worse, because the radial scale is larger. In addition new constraints are:

6) Power consumption increase by $\times 2$.

7) Loss of momentum measurement on 1/3 of azimuth, together with particle correlations in this region.

8) Likely cost increase.

The relative weighting of these advantages and disadvantages still seems to favor a solenoidal configuration, primarily because of the relative weighting between 2) and 7). There has been no design which clearly removes the constraints 2), 5), and 7) simultaneously. This is not to say it is impossible,and other alternatives should be pursued.

### C. Streamer Chamber As Central Detector

The Cerenkov and TOF counters of the detector described in Sec. III can be combined with different central detectors providing the angle and momentum determination. An interesting possibility for this central detector appears to be a streamer chamber (SC), since it combines

1) large solid angle ( $\gtrsim 0.85 \times 4\pi$),

2) high spatial resolution (setting error $\simeq 100\,\mu$) and high sampling density ($\approx 2.5$ streamers/cm),

3) the possibility of particle identification by ionization measurement for $p \lesssim 1$ GeV/c, where most of the particles are to be expected.

A SC in an axial field is discussed elsewhere in this in this summer study. We outline here only some implications of the installment of a SC into the high momentum detector described above: For good $\Delta p/p$ the electric field of the SC has to be applied parallel to the magnetic field, i.e., in beam direction. Therefore the photography has to be done in the beam direction. This requires that the pole pieces of the magnet be taken out to provide an optically free path in the front- and end-plate of the magnet.

The present magnet would allow for a central SC of about 1.6 m diameter. Taking into account an inner free space of 0.3 m diameter for beam pipe, trigger counters, and HV insulation of the SC from the beam pipe,

the minimum track length would amount to 0.65 m. For a $\Delta p/p \simeq 10\%$ at 10 GeV/c an average field over the SC of about 5 kG would be required.

A SC central detector appears to be extremely attractive for the very rare high momentum processes, since it can cover a larger solid angle than a wire chamber central detector and provides a maximum of information with respect to pattern recognition and particle identification. A converter plate of 1-2 radiation lengths in the chamber would in addition allow counting of photons accompanying charged hadrons.

## V. USEFUL DETECTION DEVICES WHICH MIGHT BE DEVELOPED

The Cerenkov counter system outlined in this report represents a compromise between identifying particles over a large solid angle and maintaining a feasible detector radius. The result is particle identification over different momentum intervals in different octants and a detector which is still inconveniently large. While this is a reasonable compromise for inclusive measurements one can easily imagine experiments (e.g., measurement of multiparticle correlation) for which more uniform identification will be necessary. We therefore consider what technical development might result in a more compact and uniform particle identification system.

Development is currently proceeding on particle identifiers which use drift chambers to measure the relativistic rise of ionization in gases above 5 GeV/c. Currently such devices are unproven and tend to be 2-5 m long. If these prove feasible and if they can be shortened to around 1 m, they would be a valuable addition to this apparatus (replacing two Cerenkov counters).

A second possibility is the use of differential Cerenkov counters. As normally constructed, these require narrowly collimated beams since Cerenkov light is only accepted over a small angular range. However, if light could be collected over a large angular range and the Cerenkov angle simultaneously measured, then the collimation requirement would disappear.

The scheme envisioned for accomplishing this is as follows: The Cerenkov light is focused onto a plane consisting of a large number of small detectors and the Cerenkov ring reconstructed after the fact. Tilting of the particle trajectory relative to the optical axis would result in an elliptical rather than a circular ring, but since the angle of the particle can be measured independently this results in no confusion. Since the particle momentum is also independently measured the particle is uniquely identified,

provided the Cerenkov rings of $\pi$, K, and p at that momentum can be resolved.

The inherent limitations of this technique arise from the smearing of the Cerenkov rings due to multiple scattering and optical dispersion in the Cerenkov radiator. To examine the first of these we consider a 1 m liquid $H_2$ Cerenkov counter, which probably has a larger density and refractive index than would be used in a realistic counter of this type. Figure 9 shows the difference between the Cerenkov angle for $\pi$, K, p and the maximum possible Cerenkov angle as a function of momentum in the region for above threshold. Also shown is the angular error to be expected from multiple scattering. It can be seen from the figure that up to 15 GeV/c multiple scattering is not a limitation for particle separation.

The limitation imposed by optical dispersion is closely related to the selection of a Cerenkov medium. This is an area in which we recommend development. The other necessary ingredient of this method is a large-area, cheap, high quantum efficiency position detector for Cerenkov photons. It is not necessary that such a device have time resolution better than $\sim 2\mu s$.

In conclusion we recommend the following areas for improvement:

(1) Development of short (< 1 m) efficient relativistic rise detector.

(2) Search for a low-dispersion Cerenkov radiator with refractive index between liquid $H_2$ (n = 1.112) and about n = 1.01. An index of n = 1.02 would be ideal.

(3) Development of a cheap large-area position-measuring Cerenkov photon detector with good space resolution and high quantum efficiency.

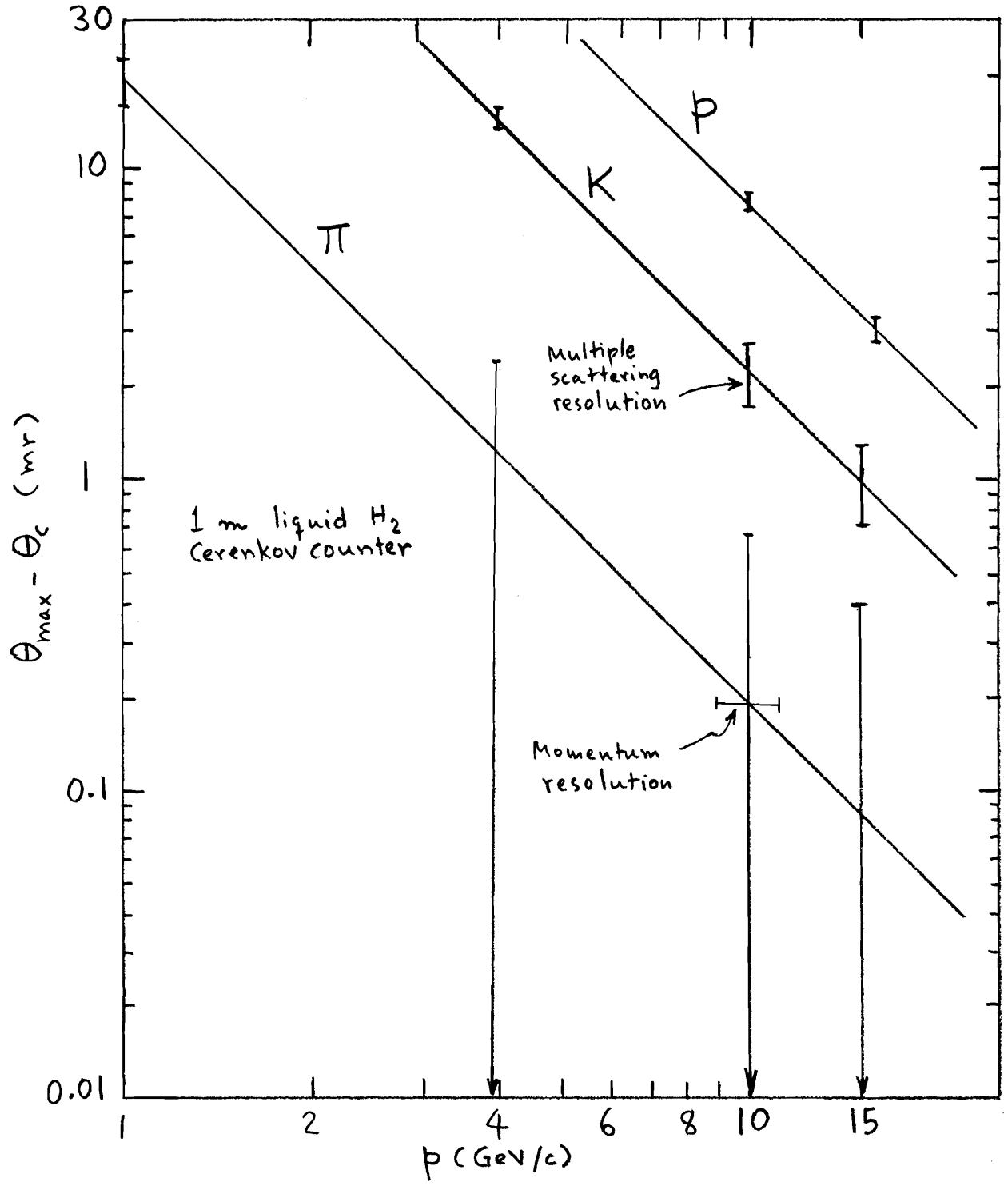


Fig. 9. Difference between Cerenkov angle, $\theta_c$, for π, K, and p and the maximum possible Cerenkov angle, $\theta_{max}$, as a function of momentum for a 1-m liquid $H_2$ Cerenkov counter.